Journal of Magnetic Resonance **141,** 44–51 (1999)
Article ID jmre.1999.1886, available online at http://www.idealibrary.com on IDEAL®

# HN($\alpha/\beta$-COCA-*J*) Experiment for Measurement of $^1J_{C'C^\alpha}$ Couplings from Two-Dimensional [$^{15}$N, $^1$H] Correlation Spectrum

Perttu Permi,*[,1] Tia Sorsa,* Ilkka Kilpeläinen,* and Arto Annila†

**Institute of Biotechnology, P.O. Box 56, University of Helsinki, FIN-00014, Helsinki, Finland; and*
*†VTT Chemical Technology, P.O. Box 1401, FIN-02044 VTT Espoo, Finland*

Received April 26, 1999; revised July 27, 1999

**A new method for measurement of one-bond $^{13}C'$–$^{13}C^\alpha$ scalar and dipolar couplings from a two-dimensional [$^{15}$N, $^1$H] correlation spectrum is presented. The experiment is based on multiple-quantum coherence, which is created between nitrogen and carbonyl carbon for simultaneous evolution of $^{15}$N chemical shift and coupling between $^{13}C'$ and $^{13}C^\alpha$. Optional subspectral editing is provided by the spin-state-selective filters. The residual dipolar dipolar contribution to the $^{13}C'$–$^{13}C^\alpha$ coupling can be measured from these simplified [$^{15}$N, $^1$H]-HSQC-like spectra. In this way, without explicit knowledge of carbon assignments, conformational changes of proteins dissolved in dilute liquid crystals can be probed conveniently, e.g., in structure activity relationship by NMR studies. The method is demonstrated with human cardiac troponin C.** © 1999 Academic Press

*Key Words:* **cTnC; dipolar coupling; multiple-quantum coherence; spin-state-selective filter.**

## INTRODUCTION

Recently found means to enhance anisotropic tumbling of solute molecules by dilute liquid crystalline media (*1–6*) have rendered residual dipolar couplings observable. The directional information obtained from dipolar couplings can be used in protein structure determination (*6–9*). This approach calls for means to measure covalently determined one-bond and two-bond couplings, which have previously been judged rather insignificant for the structure determination compared with three-bond couplings related to dihedral angles. Nevertheless, the $^1J_{C^\alpha H^\alpha}$ and $^1J_{NC^\alpha}$ scalar couplings have been found to correlate with protein's secondary structure (*10, 11*) as well as $^1J_{C'N}$, which is also sensitive to hydrogen bonding (*12*). Accordingly, there are various methods to measure, for example, $^1J_{C^\alpha H^\alpha}$, $^1J_{NC^\alpha}$, $^1J_{C'N}$, $^1J_{C'C^\alpha}$, and $^1J_{NH}$ coupling constants in proteins (*10–16*).

There are spectroscopic reasons in favor of measuring couplings from [$^{15}$N, $^1$H] correlation spectra: (1) Among the nuclei in the backbone of proteins, usually amide protons and nitrogens provide the best dispersion of chemical shifts, that is, minimal cross peak overlap. (2) Transverse relaxation rates of amide nitrogen and proton in protonated samples are slower than corresponding rates of aliphatic carbons and protons. Furthermore, transverse relaxation optimized spectroscopy (TROSY), which exploits the destructive relaxation interference between $^{15}$N chemical shift anisotropy (CSA) and $^{15}$N–$^1$H dipolar interaction, offers significant improvement in resolution and sensitivity at high magnetic fields (*17–20*). (3) Heteronuclear polarization transfer steps are easier to control more precisely with nitrogen than with carbon because there is no significant coupling between nitrogens in the polypeptide backbone. (4) Water signal can be effectively suppressed without disturbing $^1H^N$ signals of the solute. There are also practical advantages in the measurement of couplings from the [$^{15}$N, $^1$H] correlation spectra. For example, in the study of structure activity relationship (SAR) by NMR (*21–23*), the [$^{15}$N, $^1$H]-HSQC (*24*) is frequently used. Amide nitrogen and proton chemical shifts are very sensitive to changes in chemical enviroment and conformation. It is also conceivable that changes of residual dipolar couplings induced by ligand binding could be observed concomitantly with chemical shift changes to reveal conformational changes.

Here we focus on the measurement of $^{13}C'$–$^{13}C^\alpha$ dipolar couplings from the [$^{15}$N, $^1$H] correlation spectra. These couplings have been previously measured from the [$^{13}$C, $^1$H]-CT-HSQC spectrum (*14*), in which the resolution in the indirect $^{13}$C-dimension is limited due to couplings of $C^\alpha$ to $C^\beta$ ($t_{1,\max}$ usually ~28 ms) and rapid transverse relaxation of $C^\alpha$. Obviously, this method is not applicable to perdeuterated proteins. These problems can be circumvented by measuring the coupling from a coupled two-dimensional H(N)CO spectrum (*15*). A limitation of this experiment is the relatively small dispersion of $^{13}C'$ resonances. Spectral crowding can be reduced by a longer 3D-version of the experiment. In this context, we considered an experiment which would allow the measurement of $^1J_{C'C^\alpha}$ scalar and dipolar couplings conveniently from spectra superficially resembling the [$^{15}$N, $^1$H]-HSQC spectrum. We describe here the gradient-selected PEP (preservation of equivalent pathways)-HSQC experiments (*25, 26*) either with or without spin-state-selective ($\alpha/\beta$) filters (*27–30*). Previously,

[1] To whom correspondence should be addressed. Fax: +358-9-708 59541. E-mail: Perttu.Permi@helsinki.fi.



1090-7807/99 $30.00
Copyright © 1999 by Academic Press
All rights of reproduction in any form reserved.

the spin-state-selective filters have been incorporated mainly into the [$^{15}$N, $^1$H] and [$^{13}$C, $^1$H]-HSQC pulse sequences (*27–30*), but also into a HN($\alpha/\beta$-NC′-$J$)-TROSY and 2D-H(N)CO experiments for the determination of $^1J_{NC'}$ and $^2J_{H^NC'}$ (*15, 16*).

## DESCRIPTION OF THE PULSE SEQUENCES

The intention is to record a two-dimensional [$^{15}$N, $^1$H] correlation spectrum, where the nitrogen chemical shift is modulated by the one-bond $^{13}C'-^{13}C^\alpha$ coupling. This can be accomplished by generation of multiple-quantum coherence between the nitrogen of residue $i$ and carbonyl carbon of residue $i$-1 and subsequently recording simultaneously nitrogen chemical shift and $^{13}C'-^{13}C^\alpha$ coupling evolution during the $t_1$ period. The chemical shift evolution of $^{13}$C′ is prevented by application of 180° pulses on carbonyl and $C^\alpha$ spins in the middle of $t_1$. We refer to this experiment as HN(COCA-$J$). The flow of coherence is

$$^1H^N \xrightarrow{J_{NH}} {}^{15}N \xrightarrow{J_{NC'}} {}^{13}C', {}^{15}N(t_1) \xrightarrow{J_{NC'}}$$

$$^{15}N \xrightarrow{J_{NH}} {}^1H^N(t_2),$$

where $t_1$ and $t_2$ are the evolution and acquisition times. Couplings used for magnetization transfer are indicated above the arrows. In the spin-state-selective experiment, referred as HN($\alpha/\beta$-COCA-$J$), an $\alpha/\beta$-half-filter element is placed prior to the $t_1$ evolution period.

The HN(COCA-$J$) pulse sequence for determination of $^1J_{C'C^\alpha}$ couplings from the [$^{15}$N, $^1$H] correlation spectrum is presented in Fig. 1A. The experiment begins with the magnetization transfer from $^1H^N$ via INEPT (*31*) to $^{15}$N antiphase coherence with respect to $^1H^N$, described by an operator $2H_zN_y$. During the subsequent delay $2*\Delta$, which is incorporated in the delay $2*T_N$, the $^{15}$N coherence rephases with respect to $^1H^N$ and WALTZ-16 (*32*) decoupling field on the proton is turned on. The $^{15}$N coherence dephases with respect to the carbonyl spin during the delay $2*T_N$ and is converted by a 90° pulse on carbonyl to a mixed double-/zero-quantum (DQ/ZQ) coherence, $2N_{x,y}C'_y$. In the middle of the following $t_1$ evolution period a 180° pulse is applied on $^{13}$C′ and $^{13}C^\alpha$. Thus, the chemical shift of nitrogen and the coupling between carbonyl and $\alpha$ carbons evolves simultaneously. This results in in-phase doublet components at $\omega_N + \pi J_{C'C^\alpha}$ and $\omega_N - \pi J_{C'C^\alpha}$ in the $F_1$-dimension. A 90° pulse at the end of $t_1$ period converts the nitrogen–carbonyl multiple-quantum coherence back into the $^{15}$N single-quantum coherence, $2N_{x,y}C'_z$. During the latter $2*T_N$ period, the antiphase nitrogen–carbonyl carbon coherence refocuses simultaneously with the nitrogen chemical shift. The proton decoupling field is switched off to allow dephasing of the $^{15}$N coherence with respect to $^1H^N$ during $2*\Delta$. Finally, the antiphase $^{15}$N coherence is transferred to $^1H^N$ by a reverse INEPT step. An additional 90° pulse on $^{13}$C′ serves to purge an undesired magnetization. A selective SEDUCE-1 (*33*) decoupling field is applied on $C^\alpha$ region during the $2*T_N$ delays to prevent dephasing of nitrogen coherence due to coupling to $^{13}C^\alpha$. Alternatively, a selective 180° pulse for $\alpha$ carbons in the middle of $2*T_N$ delays could be used to refocus dephasing nitrogen coherence.

In the $\alpha/\beta$-filtered experiment, presented in Fig. 1B, the initial magnetization transfer from $^1H^N$ spin to the antiphase $^{15}$N spin coherence is identical to the HN(COCA-$J$) experiment. However, the HMQC-like coherence transfer from $^{15}$N to $^{13}$C′ in the HN(COCA-$J$) experiment is replaced now by the INEPT step. Consequently, the antiphase $^{13}$C′ coherence with respect to $^{15}$N is generated. The subsequent $\alpha/\beta$-half-filter element generates either antiphase or in-phase $^{13}C'-^{13}C^\alpha$ coherence described by the operators $4N_zC'_xC^\alpha_z$ and $2N_zC'_y$, respectively. A mixed DQ/ZQ coherence is created with a 90° pulse on nitrogen prior to the $t_1$ evolution period. In the case of antiphase $\alpha/\beta$-filter, the phase of the $^{15}$N 90° pulse is shifted by 90° with respect to the in-phase spectrum and simultaneously an in-phase $^{13}$C′ coherence is purged by a 90° pulse on carbonyl (pulses denoted with filled bars are applied in this case). This ensures absorptive antiphase lineshape in the $F_1$-dimension as dispersive contribution arising from $J$ mismatch is removed and will not be converted into detectable proton magnetization at the end of the pulse sequence. Analogous to the HN(COCA-$J$) experiment, the nitrogen chemical shift is incremented simultaneously with the one-bond $^{13}C'-^{13}C^\alpha$ coupling evolution during $t_1$. In the case of in-phase $\alpha/\beta$-filter, cosine modulated absorptive in-phase lines are generated (pulses denoted with unfilled bars are applied on $C^\alpha$, together with the 180° pulse on C′). In summary, the signal of interest in the antiphase spectrum is proportional to $N_{x,y}C'_y\sin(\omega_N t_1)\sin(\pi J t_1)$ and in the in-phase spectrum to $N_{x,y}C'_y\cos(\omega_N t_1)\cos(\pi J t_1)$. After the $t_1$ evolution period, the antiphase nitrogen single-quantum coherence, $2N_{x,y}C'_z$, is regenerated by a 90° pulse on carbonyl and is allowed to refocus simultaneously with dephasing of nitrogen–proton coherence as in the HN(COCA-$J$) experiment. A simultaneous 90° pulse on carbonyl is used to purge undesired dispersive magnetization terms. Finally, the magnetization is transferred from $^{15}$N to $^1H^N$ by the reverse INEPT step.

Quadrature detection and coherence selection in both experiments are obtained by gradient selection combined with sensitivity enhancement via the preservation of equivalent pathways. Postacquisitional addition and subtraction of these data sets and their corresponding quadrature counterparts result in spectra with high-field and low-field doublet components at $\omega_N + \pi J_{C'C^\alpha}$ and $\omega_N - \pi J_{C'C^\alpha}$ in the $F_1$-dimension, respectively.

It should be noted that the spin-state-selective experiment could be easily converted into a three-dimensional HNCO($\alpha$/

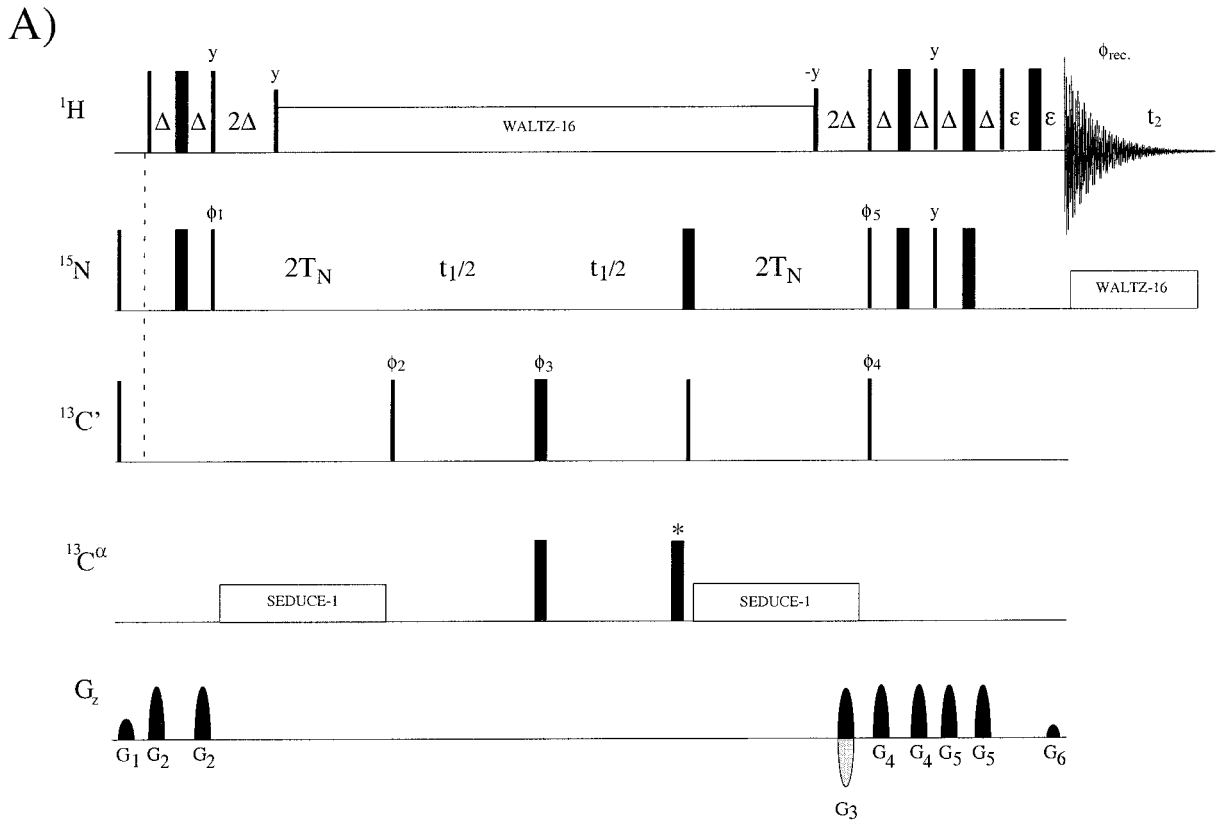
A)
$^1$H
$^{15}$N
$^{13}$C'
$^{13}$C$^\alpha$
G$_z$
WALTZ-16
SEDUCE-1
2T$_N$
t$_1$/2
G$_1$ G$_2$ G$_2$ G$_3$ G$_4$ G$_4$ G$_5$ G$_5$ G$_6$

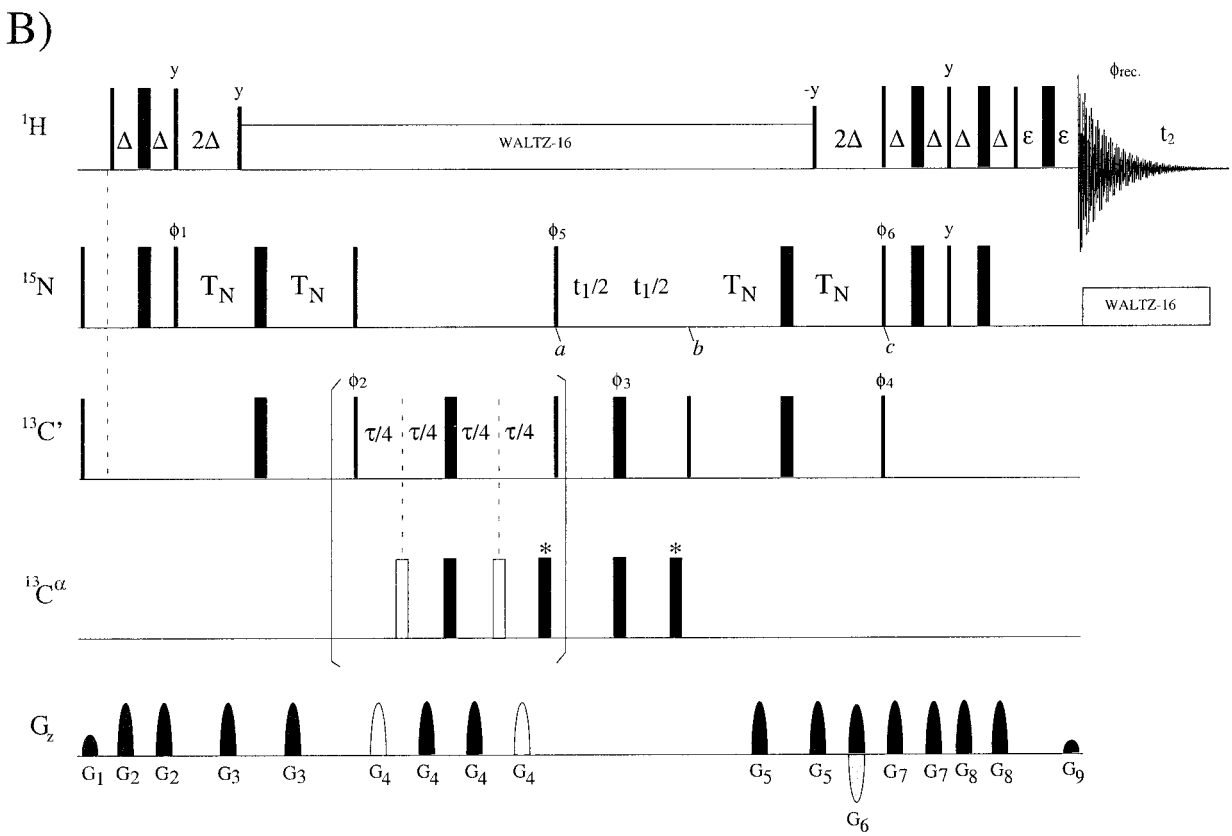
B)
$^1$H
$^{15}$N
$^{13}$C'
$^{13}$C$^\alpha$
G$_z$
WALTZ-16
T$_N$
t$_1$/2
τ/4
G$_1$ G$_2$ G$_2$ G$_3$ G$_3$ G$_4$ G$_4$ G$_4$ G$_4$ G$_5$ G$_5$ G$_6$ G$_7$ G$_7$ G$_8$ G$_8$ G$_9$

$\beta$-COCA-$J$) experiment, in order to decrease resonance overlap in the case of larger proteins. The 3D experiment is obtained by removing the 180°($^{13}C'/^{13}C^\alpha$) pulses from the $t_1$ period and replacing them with a 180° pulse on nitrogen. The 90°($^{15}N$) pulse before the $t_1$ period should then be placed after the $t_1$ period and the $^{15}N$ chemical shift is incremented in a constant-time manner during the latter $2*T_N$ period. A more detailed description of the modification is given in the legend to Fig. 1B. Alternatively, a two-dimensional [$^1H$, $^{13}C'$] experiment may be used. However, the gradient-selected sensitivity enhancement method cannot be invoked in the case of the 2D-H(N)CO($\alpha/\beta$-COCA-$J$) experiment.

## RESULTS AND DISCUSSION

The $\alpha/\beta$-half-filters are prone to a $J$ crosstalk when coupling evolution does not match the filter period. The $J$ crosstalk deteriorates subspectral editing, that is, in addition to the desired principle multiplet component, the minor component from the other spin state will be present in the subspectra. The intensity ratio of the principle component to the minor component in this case is

$$\frac{1 + \sin(\pi J\tau)}{1 - \sin(\pi J\tau)} = \frac{I_p}{I_m}, \qquad [1]$$

where $J$ is the true coupling constant and $\tau$ is the delay of the filter. $I_p$ and $I_m$ are the intensities of the principle and minor components, respectively.

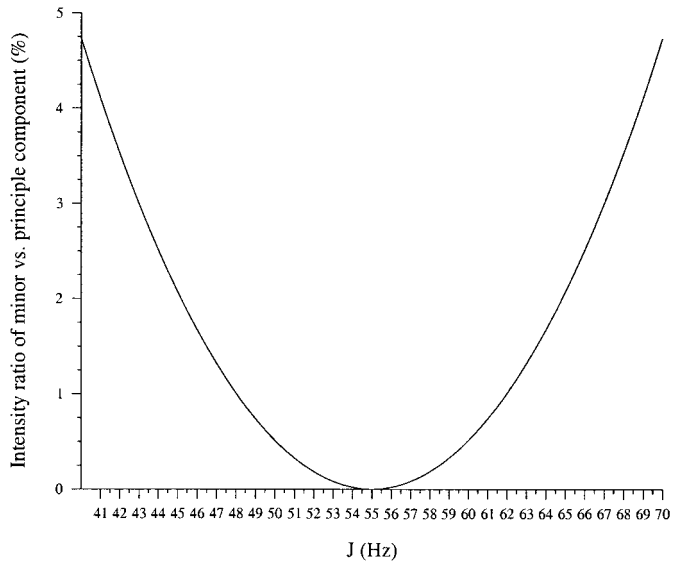


**FIG. 2.** Intensity (%) of the minor component relative to the principle component as a function of $J$. The curve was calculated with Eq. [1] using a $\tau$ value of 9.09 ms, corresponding to 55 Hz taken as the average value for $^1J_{C'C^\alpha}$.

The intensity ratio of the minor component to the principle component as a function of $J$ is shown in Fig. 2. For the $^{13}C'-^{13}C^\alpha$ coupling, a good filtration can be achieved. For a

**FIG. 1.** (A) HN(COCA-$J$) pulse sequence for the measurement of $^1J_{C'C^\alpha}$ couplings from [$^{15}N$, $^1H$] correlation spectrum. Hard 90° and 180° pulses are marked by narrow and wide bars, respectively, with phase $x$, unless indicated otherwise. All spectra were recorded on a Varian Unity 600 MHz spectrometer equipped with a pulsed field gradient unit and a triple-resonance probe with an actively shielded $z$-axis gradient. The $^1H$ carrier was placed at the $H_2O$ frequency, the $^{15}N$ carrier was set to the center of $^{15}N$ spectral region (119 ppm), and the $^{13}C'$ carrier was set to the center of the $^{13}C'$ spectral region (179 ppm). The WALTZ-16 sequence (*32*) was used to decouple $^1H$ during heteronuclear coherence transfer and $^{15}N$ during acquisition. $^{13}C$ 90° (180°) pulses were applied with a strength of $\delta/\sqrt{15}$ ($\delta/\sqrt{3}$), where $\delta$ is the frequency between centers of the $^{13}C'$ and $^{13}C^\alpha$ regions. All $^{13}C'$ pulses were applied on-resonance and $^{13}C^\alpha$ pulses off-resonance with phase modulation by $\delta$. The off-resonance compensation pulses (*36*) are indicated with asterisks. Phase cycling: $\phi_1 = x, -x$; $\phi_2 = x, x, -x, -x$; $\phi_3 = 4(x), 4(y), 4(-x), 4(-y)$; $\phi_4 = 16(x), 16(-x)$; $\phi_{rec} = 4(x, -x, -x, x, -x, x, x, -x)$. Delay durations: $\Delta = 1/(2J_{NH})$, $T_N = 1/(4J_{NC'})$, $\epsilon$ = gradient + field recovery delay. Gradient strengths (durations): $G_1$ = 4 G/cm (0.7 ms), $G_2$ = 12 G/cm (0.7 ms), $G_3$ = 18 G/cm (2.5 ms), $G_4$ = 8 G/cm (0.7 ms), $G_5$ = 15.6 G/cm (0.7 ms), $G_6$ = 17.410 G/cm (0.25 ms). Frequency discrimination in $F_1$ is obtained using the PEP sensitivity-enhanced gradient selection (*25, 26*). The echo and anti-echo signals are collected separately by inverting the sign of the $G_3$ gradient pulse together with the inversion of $\phi_5$. In addition to echo/anti-echo selection, $\phi_1$ and $\phi_{rec}$ are incremented according to the States-TPPI protocol (*42*). (B) HN($\alpha/\beta$-COCA-$J$) pulse sequence of $\alpha/\beta$-half-filtered experiment for the measurement of $^1J_{C'C^\alpha}$ couplings from two [$^{15}N$, $^1H$] correlation subspectra. The phase cycling for data modulated by $\cos(\omega_N t_1)\cos(\pi J_{C'C^\alpha} t_1)$: $\phi_1 = x, -x$; $\phi_2 = x, x, -x, -x$; $\phi_3 = 4(x), 4(y), 4(-x), 4(-y)$; $\phi_4 = 16(x), 16(-x)$; $\phi_5 = x$; $\phi_{rec} = 4(x, -x, -x, x, -x, x, x, -x)$. The phase $\phi_5$ is incremented by 90° for the data modulated by $\sin(\omega_N t_1)\sin(\pi J_{C'C^\alpha} t_1)$. The cosine and sine modulated data sets are collected in an interleaved manner. Delay durations as in (A), except for $\tau = 1/(2J_{C'C^\alpha})$. The $F_1$-quadrature is achieved as in (A). The echo and anti-echo signals are collected separately by inverting the sign of the $G_6$ gradient pulse along with the inversion of $\phi_6$. Additionally, for each $t_1$ value, the phases $\phi_5$ and $\phi_{rec}$ are incremented by 180°. Gradient strengths (durations): $G_1$ = 4 G/cm (0.7 ms), $G_2$ = 12 G/cm (0.7 ms), $G_3$ = 5 G/cm (0.7 ms), $G_4$ = 5 G/cm (0.7 ms), $G_5$ = 11 G/cm (0.7 ms), $G_6$ = 18 G/cm (2.5 ms), $G_7$ = 8 G/cm (0.7 ms), $G_8$ = 15.6 G/cm (0.7 ms), and $G_9$ = 17.410 G/cm (0.25 ms). Water suppression by water-flip-back (*43, 44*) can be implemented into the pulse sequences, e.g., between the second 90°($^1H$) and the 90°$_{\phi 1}$($^{15}N$) pulses. Scheme for measuring $^1J_{C'C^\alpha}$ in 3D-HNCO($\alpha/\beta$-COCA-$J$) experiment. The 180°($^{13}C$) pulses during $t_1$ (between time points $a$ and $b$) are replaced with the 180° ($^{15}N$) pulse applied at the midpoint of $t_1$, and the 90°$_{\phi 5}$($^{15}N$) pulse at position $a$ is omitted and applied at position $b$ instead. Hence, the density operators of interest immediately after point $a$ for the in- and antiphase spectrum are $2N_zC'_y$ and $4N_zC'_xC^\alpha_z$, respectively. Phase cycling for $\cos(\omega_{C'} t_1)\cos(\pi J_{C'C^\alpha} t_1)$ modulated data: $\phi_1 = x, -x$; $\phi_2 = x, x, -x, -x$; $\phi_4 = x, x, x, x, -x, -x, -x, -x$; $\phi_5 = x$; $\phi_{rec} = x, -x, -x, x$. For $\sin(\omega_{C'} t_1)\sin(\pi J_{C'C^\alpha} t_1)$ modulated data, the 90°($^{13}C'$) pulse at position $b$ is applied with phase $y$. The $^{13}C'$ pulses in the $\alpha/\beta$-filter element are altered according to the States-TPPI protocol to obtain quadrature in $t_1$. The latter $2*T_N$ period between the time points $b$ and $c$ is replaced with the usual $^{15}N$ constant time evolution ($T_N - t_2/2$ 180°($^{15}N/^{13}C'$) $T_N + t_2/2$) period, and the semiselective $C^\alpha$-decoupling is applied during this period using, e.g., SEDUCE-1 decoupling field. After addition and subtraction of these two data sets, two spectra are generated with the upfield and downfield doublet components at $\omega_{C'} - \pi J_{C'C^\alpha}$ and $\omega_{C'} + \pi J_{C'C^\alpha}$ in the $F_1$-dimension.

values deviating up to ±10 Hz from the filter tuned to 55 Hz, the intensity of the minor component will be at least 30 times smaller compared with the intensity of the principle component. This is sufficient to separate the $\alpha$- and $\beta$-states clearly into two subspectra also when there is an additional variation in the $^{13}C'-^{13}C^{\alpha}$ coupling due to residual dipolar couplings. In practice the $^{13}C'-^{13}C^{\alpha}$ dipolar coupling may vary up to ±5 Hz. This corresponds approximately to ±25 Hz in $^{15}N-^{1}H^{N}$ coupling and larger dipolar contributions would limit the polarization transfer. The effects of *J* crosstalk to the measured couplings have been addressed earlier (*16, 27–30, 34, 35*). In this case of relatively large splitting between the $\alpha$- and $\beta$-states of doublet components compared with their line widths, the *J* crosstalk is only harmful when the minor component of one residue distorts the line of the principle component of another residue and leads to a distorted signal and a slightly erroneous measurement of the coupling constant. The deviation from the true coupling depends on the size and degree of overlap of the minor component relative to the principle component.

Also the relaxation of $^{13}C^{\alpha}$ spin can lead to an insufficient $\alpha/\beta$-filtration, because of different relaxation rates for the in-phase and antiphase coherences. Thus, neglecting other relaxation mechanisms, the in-phase and antiphase operators relax at rates given by Eq. [2],

$$R_2(N_z C_y') = R_2(^{13}C') + R_1(^{15}N);$$
$$R_2(N_z C_x' C_z^{\alpha}) = R_2(^{13}C') + R_1(^{13}C^{\alpha}) + R_1(^{15}N). \qquad [2]$$

Consequently, the intensity of the in-phase doublet differs from that of the antiphase doublet. Effects of differential relaxation rates can be corrected, for example, by scaling the in- and antiphase signals before construction of the subspectra or by taking an appropriate linear combination of the in- and antiphase spectra (*15, 34, 35*). In practice, using an average scaling factor for all signals will largely improve the ratio of the principle to the minor component, but of course, variation in the relaxation rates for different residues depending on the internal protein dynamics will cause residual artifacts. In any case, there is a possibility of suppressing the *J* crosstalk for individual resonances by reprocessing for the refined linear combination of equivalent regions of the subspectra.

The off-resonance effect of the 180($^{13}C^{\alpha}$) pulses on $^{13}C'$ was compensated for during the $t_1$ period and also in the antiphase filter element by applying an additional compensatory pulse on $^{13}C^{\alpha}$ (*36*). Alternatively, a constant phase offset to the 180°($^{13}C'$) pulse could be used. It is noteworthy that the state-of-the-art probes, with the usual composite pulse element ($90_x180_y90_x$), are able to invert (>97%) carbonyl carbons, while a proper refocusing of the $^{13}C^{\alpha}$ chemical shifts is achieved (*37*). We did not try to use this approach, however. Additionally, utilization of shaped pulses, e.g., REBURP or G3 (*38, 39*), for refocusing and inversion could also improve the performance.

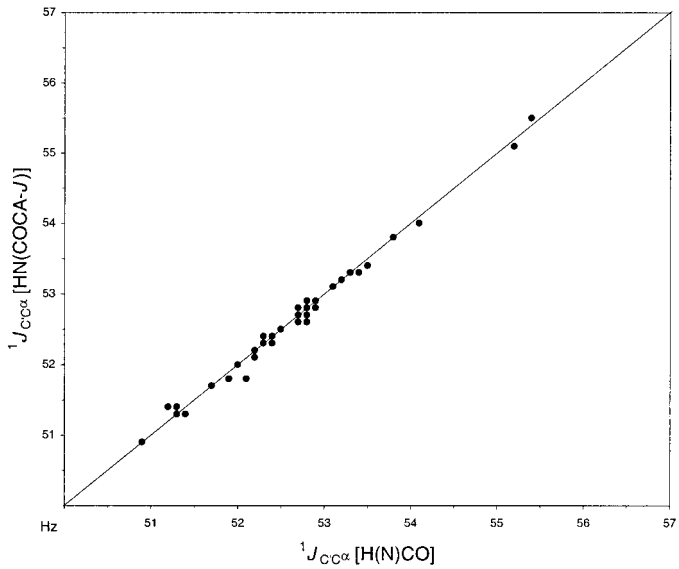


**FIG. 3.** Correlation of $^{1}J_{C'C^{\alpha}}$ coupling constants measured from spectra acquired with the H(N)CO vs HN(COCA-*J*) experiments. The pairwise root-mean-squared deviation is 0.09 Hz. The couplings were derived from in-phase splittings measured from 1 mM uniformly $^{15}N/^{13}C$-labeled ubiquitin (VLI Reseach Inc. Southeastern, PA) in 90%/10% $H_2O/D_2O$, pH 5.8, 50 mM sodium phosphate buffer in water at 25°C.

It is well known that in the presence of cross-correlation between dipole–dipole (DD) and chemical shift anisotropy interactions, two doublet components relax at different rates (*40*). Both the in- and the antiphase filter elements are designed to minimize effects of this interference between $^{13}C'$ CSA and $^{13}C'-^{13}C^{\alpha}$ DD by averaging the relaxation rates of doublet components by the inversion of $^{13}C^{\alpha}$'s spin states during the filter elements (*30*). This also largely prevents a formation of spurious terms arising from the interference between $^{13}C'-^{15}N$ and $^{13}C'-^{13}C^{\alpha}$ dipolar interactions (*41*).

The pulse sequences were tested with the regulatory domain of human cardiac troponin C (cTnC, 10 kDa, 93 amino acid residues) dissolved in both isotropic and anisotropic phase. In addition, results obtained from human ubiquitin (8.6 kDa, 76 residues) in water at 25°C using the HN(COCA-*J*) pulse sequence, shown in Fig. 1A, were compared with those obtained under similar conditions with the $^{13}C^{\alpha}$-coupled 2D-H(N)CO experiment (no spectra are shown).

There is a good agreement between the values obtained using these two methods. The pairwise root-mean-squared deviation is less than 0.1 Hz for the 51 residues considered, i.e., residues with no significant cross peak overlap in either spectrum. Figure 3 shows the correlation between the measured $^{1}J_{C'C^{\alpha}}$ splittings obtained with the HN(COCA-*J*) and H(N)CO experiments. Figure 4 presents an expansion of the [$^{15}N$, $^{1}H$] correlation spectrum of cTnC dissolved in water. Figure 4A serves for a reference and shows both the upfield and the

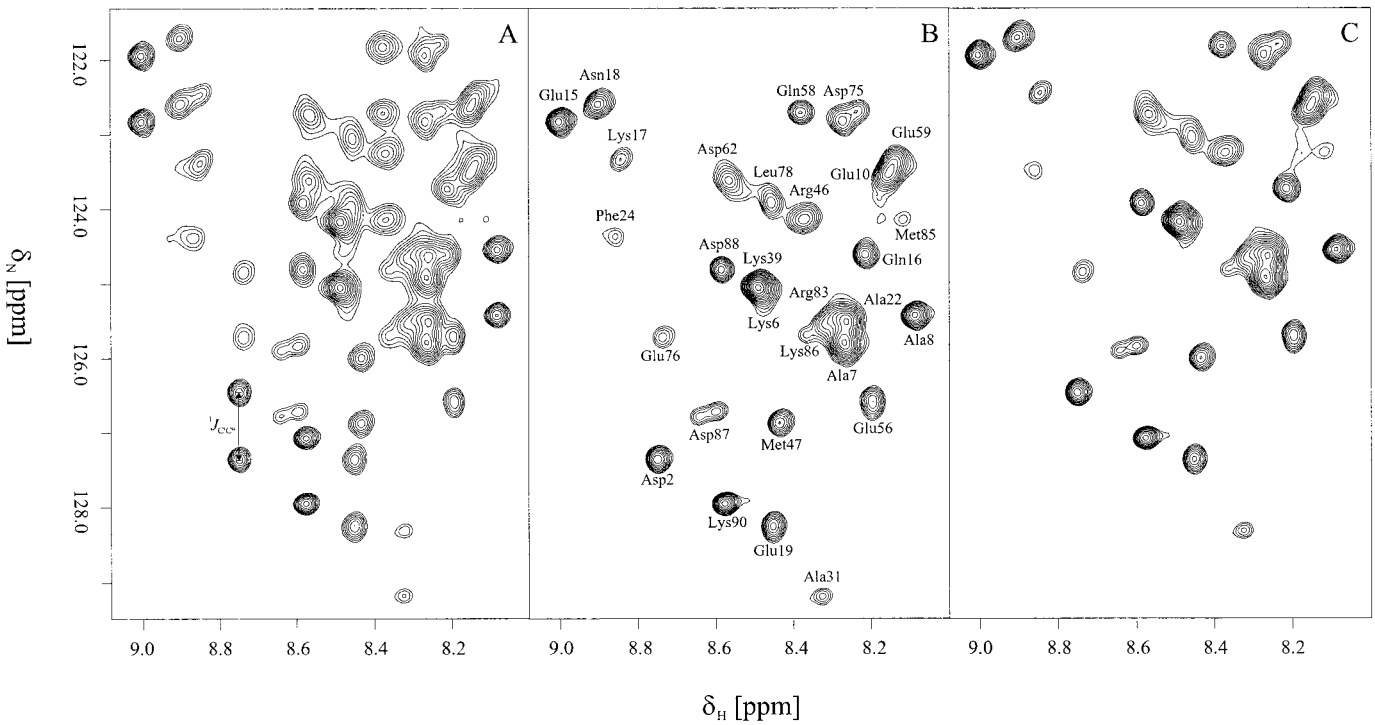


**FIG. 4.** Representative expansions of the HN($\alpha/\beta$-COCA-$J$) and HN(COCA-$J$) spectra obtained from 1.0 mM uniformly $^{15}N/^{13}C$ enriched 1:1 cTnC/TnI protein complex, measured at 600 MHz, 93%/7% $H_2O/D_2O$, pH 6.0, 40°C, using pulse sequences in Fig. 1. The HN(COCA-$J$) spectrum is provided for a reference showing both doublet components in-phase (A), acquired with the experiment in Fig. 1A. Downfield and upfield doublet components are shown separately in (B) and (C), respectively, as obtained after postacquisitional addition and subtraction of the data sets recorded with experiment B. Experimental parameters for the HN(COCA-$J$) and HN($\alpha/\beta$-COCA-$J$) experiments: Spectral widths in the $F_1$ ($F_2$)-dimension = 1800 (7994) Hz, number of $t_1$ increments = 256 (142 ms), acquisition time ($t_2$) = 128 ms, number of scans = 32. Data were zero-filled to 2K (4K) in the $F_1$ ($F_2$)-dimension.

downfield doublet components in-phase, recorded with the HN(COCA-$J$) pulse sequence. The downfield and upfield $^{13}C'-^{13}C^\alpha$ doublet components are shown in Figs. 4B and 4C, respectively, obtained from a data set collected with the HN($\alpha/\beta$-COCA-$J$) pulse sequence given in Fig. 1B. Doublet components are clearly separated and no significant $J$ crosstalk is present in either subspectrum.

Table 1 lists some of the 74 $^1J_{C'C^\alpha}$ coupling constants measured from the regulatory domain of cTnC (89 observable $H^NN$ correlations) using the HN($\alpha/\beta$-COCA-$J$) pulse sequence. Since cTnC is a mostly helical protein, the dispersion of resonances is somewhat poor (Fig. 4) and 60 coupling values could be extracted from the corresponding nonfiltered HN(COCA-$J$) spectrum with twice as many correlations. Therefore the applicability of the nonfiltered HN(COCA-$J$) experiment is limited for larger proteins.

The sensitivity gain of the nonfiltered experiment owing to the shorter duration and fewer radiofrequency pulses compared with the filtered experiment is nevertheless rather small. The transverse relaxation time in the form of $^{13}C'$ single-quantum coherence is relatively long compared with the length of the $\alpha/\beta$-filter element (~9 ms). In our hands, the difference in sensitivity between these two experiments was 7–15% at 600 MHz $^1H$ frequency. At the highest magnetic fields the difference will be larger. For larger proteins, it may be necessary to make use of the three-dimensional $\alpha/\beta$-filtered, 3D-HNCO($\alpha/\beta$-COCA-$J$) experiment (see Fig. 1 legend), in which the $^1J_{C'C^\alpha}$

**TABLE 1**

**$^1J_{C'C^\alpha}$ Coupling Constants for Some Residues of cTnC Measured from the Spectrum Collected with the HN($\alpha/\beta$-COCA-$J$) Experiment**

| Residue | $^1J_{C'C^\alpha}$ [Hz] | Residue | $^1J_{C'C^\alpha}$ [Hz] |
|---|---|---|---|
| Met1 | 53.5 | Arg46 | 52.5 |
| Asp2 | 52.6 | Gln50 | 53.9 |
| Ala7 | 52.5 | Pro52 | 52.0 |
| Glu10 | 52.8 | Pro54 | 55.2 |
| Gln11 | 52.4 | Leu57 | 53.7 |
| Leu12 | 52.6 | Glu59 | 52.6 |
| Thr13 | 52.1 | Asp62 | 52.1 |
| Glu14 | 53.8 | Asp67 | 53.3 |
| Gln16 | 52.9 | Asp73 | 51.9 |
| Lys17 | 53.4 | Leu78 | 53.4 |
| Asn18 | 53.1 | Lys86 | 52.6 |
| Phe20 | 52.7 | Asp87 | 52.8 |
| Phe24 | 53.4 | Asp88 | 53.0 |
| Gly30 | 53.4 | Ser89 | 52.4 |
| Gly34 | 53.4 | Lys90 | 52.8 |

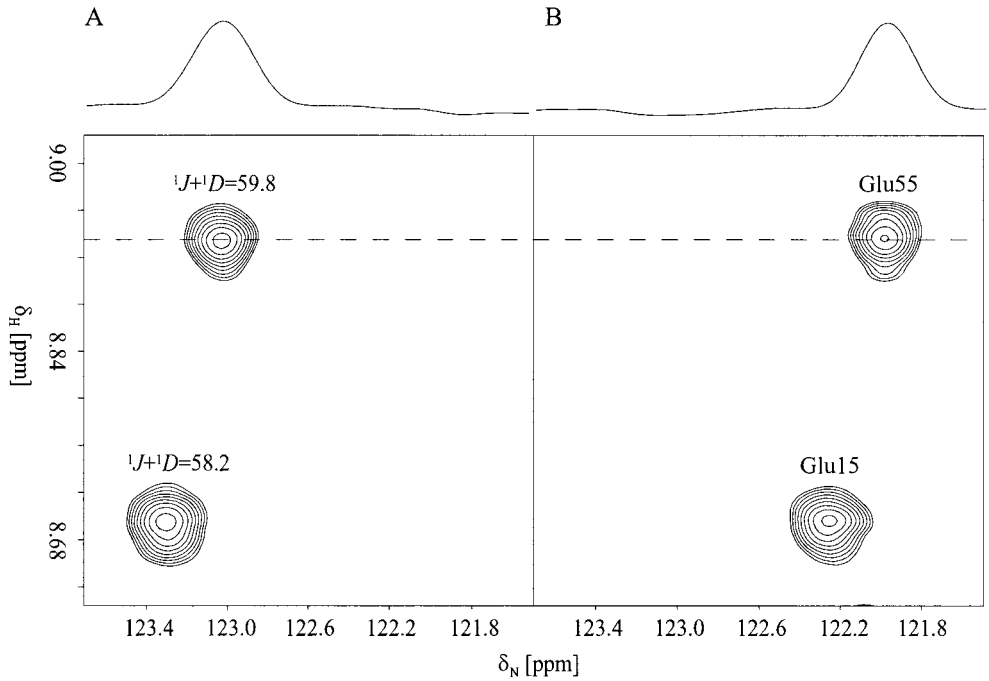


**FIG. 5.** Expansion of the HN($\alpha/\beta$-COCA-*J*) spectrum recorded from cTnC dissolved in a dilute liquid crystal. Downfield (A) and upfield (B) multiplet components are shown separately. The dashed line indicates the location of the cross-section shown. Measured $^{13}C'-^{13}C^{\alpha}$ splittings in the anisotropic phase composed of Pf1 filamentous phages (30 mg/ml) are marked in the spectrum (A). Sample conditions: 0.3 mM uniformly $^{15}N/^{13}C$ enriched cTnC protein, measured at 600 MHz, 93%/7% $H_2O/D_2O$, pH 6.5, 40°C. Experimental parameters were the same as in Fig. 4 except the number of $t_1$ increments = 128 (71 ms) and number of scans = 256. Data were zero-filled to 2K (4K) in the $F_1$ ($F_2$)-dimension; squared cosine window functions were applied in the $F_1$- and $F_2$-dimensions.

coupling and $^{13}C'$ chemical shift are detected under the $^{13}C'$ single-quantum coherence during $t_1$. After addition and subtraction of the in- and antiphase data sets, this experiment generates two HNCO-type spectra with correlations at $\omega_{C'}(i) + \pi J_{C'C^{\alpha}} t_1$, $\omega_N(i+1)$, $\omega_{HN}(i+1)$, and $\omega_{C'}(i) - \pi J_{C'C^{\alpha}} t_1$, $\omega_N(i+1)$, $\omega_{HN}(i+1)$, and thus provides a spectrum with minimal resonance overlap. The HN($\alpha/\beta$-COCA-*J*) pulse sequence was also tested with cTnC dissolved in a dilute liquid crystal, composed of filamentous phage particles (*4*). Figure 5 illustrates upfield (A) and downfield (B) doublet components of the HN($\alpha/\beta$-COCA-*J*) spectrum for two resonances in the anisotropic phase. Substantial deviation from the scalar $^1J_{C'C^{\alpha}}$ splitting can be seen for Glu14 and Pro54 residues, where dipolar contributions to the couplings are 4.4 and 4.6 Hz, respectively. The dashed line in Fig. 5 indicates the location of corresponding cross-section shown in Figs. 5A and 5B. Artifacts due to the *J* crosstalk are very small in both subspectra, implying that distortions in lineshapes in the case of resonance overlap contribute only very little to the measurement of *J* according to the Eq. [1].

In summary, we have presented a method to measure $^{13}C'-^{13}C^{\alpha}$ scalar and dipolar couplings conveniently from the two-dimensional [$^{15}N$, $^1H$] correlation spectra with or without spin-state-selective filtering. In the former case, each subspectrum contains no more cross peaks than the [$^{15}N$, $^1H$]-HSQC spectrum. Furthermore, the HN($\alpha/\beta$-COCA-*J*) scheme can be easily converted into the 3D-HNCO($\alpha/\beta$-COCA-*J*) experiment, if the dispersion of resonances in the [$^{15}N$, $^1H$] correlation spectrum is otherwise insufficient. The filter is quite insensitive to the *J* mismatch within the expected variation of $^{13}C'-^{13}C^{\alpha}$ coupling. Measurement of other one- and two-bond couplings such as $^1J_{NH}$, $^1J_{NC'}$, $^1J_{NC^{\alpha}}$, $^1J_{C^{\alpha}C^{\beta}}$, $^2J_{NC^{\alpha}}$, $^2J_{HNC'}$, and $^2J_{HNC^{\alpha}}$ from the two-dimensional [$^{15}N$, $^1H$] HSQC-type spectra acquired from samples dissolved both in water and in dilute liquid crystal provide conveniently a wealth of residual dipolar couplings from internuclear vectors at various orientations. More reliable information of protein structure can be retrieved with the constructive use of several dipolar couplings corresponding to nonredundant internuclear directions. In this way conformational changes induced by ligand binding can be observed concomitantly with chemical shift changes, e.g., in SAR by NMR studies.

## ACKNOWLEDGMENTS

We thank K. Pääkkönen and S. Heikkinen for useful discussions. This work has been supported by the Academy of Finland.

## REFERENCES

1. C. R. Sanders and J. P. Schwonek, *Biochemistry* **31,** 8898 (1992).
2. J. A. Losonczi and J. H. Prestegard, *J. Biomol. NMR* **12,** 447, (1998).

*3.* J. Struppe and R. R. Vold, *J. Magn. Reson.* **135,** 541 (1998).

*4.* M. R. Hansen, L. Mueller, and A. Pardi, *Nat. Struct. Biol.* **12,** 1065 (1998).

*5.* G. M. Clore, M. R. Starich, and A. M. Gronenborn, *J. Am. Chem. Soc.* **120,** 10571 (1998).

*6.* N. Tjandra and A. Bax, *Science* **278,** 1111 (1997).

*7.* J. R. Tolman, J. M. Flanagan, M. A. Kennedy, and J. H. Prestegard, *Proc. Natl. Acad. Sci. USA* **92,** 9279 (1995).

*8.* N. Tjandra, J. G. Omichinski, A. M. Gronenborn, G. M. Clore, and A. Bax, *Nat. Struct. Biol.* **4,** 732 (1997).

*9.* G. M. Clore and A. M. Gronenborn, *Curr. Opin. Chem. Biol.* **2,** 564 (1998).

*10.* G. W. Vuister, F. Delaglio, and A. Bax, *J. Biomol. NMR* **3,** 67 (1993).

*11.* F. Delaglio, D. A. Torchia, and A. Bax, *J. Biomol. NMR* **1,** 439 (1991).

*12.* N. Juranic, P. K. Ilich, and S. Macura, *J. Am. Chem. Soc.* **117,** 405 (1995).

*13.* J. R. Tolman and J. H. Prestegard, *J. Magn. Reson. B* **112,** 269 (1996).

*14.* G. W. Vuister and A. Bax, *J. Biomol. NMR* **2,** 401 (1992).

*15.* M. Ottiger, F. Delaglio, and A. Bax, *J. Magn. Reson.* **131,** 373 (1998).

*16.* P. Permi, S. Heikkinen, I. Kilpeläinen, and A. Annila, *J. Magn. Reson.* **140,** 32 (1999).

*17.* K. Pervushin, R. Riek. G. Wider, and K. Wüthrich, *Proc. Natl. Acad. Sci. USA* **94,** 12366 (1997).

*18.* M. Saltzmann, K. Pervushin, G. Wider, H. Senn, and K. Wüthrich, *Proc. Natl. Acad. Sci. USA* **95,** 13585 (1998).

*19.* P. Andersson, A. Annila, and G. Otting, *J. Magn. Reson.* **133,** 364 (1998).

*20.* M. Czisch and R. Boelens, *J. Magn. Reson.* **134,** 158 (1998).

*21.* P. J. Hajduk, R. P. Meadows, and S. W. Fesik, *Science* **278,** 497 (1997).

*22.* S. B. Shuker, P. J. Hajduk, R. P. Meadows, and S. W. Fesik, *Science* **274,** 1531 (1996).

*23.* S. W. Fesik, *J. Biomol. NMR* **3,** 261 (1993).

*24.* G. Bodenhausen and D. J. Ruben, *Chem. Phys. Lett.* **69,** 185 (1980).

*25.* L. E. Kay, P. Keifer, and T. Saarinen, *J. Am. Chem. Soc.* **114,** 10663 (1992).

*26.* A. G. Palmer III, J. Cavanagh, P. E. Wright, and M. Rance, *J. Magn. Reson.* **93,** 151 (1991).

*27.* A. Meissner, J. Ø. Duus, and O. W. Sørensen, *J. Biomol. NMR* **10,** 89 (1997).

*28.* A. Meissner, J. Ø. Duus, and O. W. Sørensen, *J. Magn. Reson.* **128,** 92 (1997).

*29.* P. Andersson, K. Nordstrand, M. Sunnerhagen, E. Liepinsh, I. Turovskis, and G. Otting, *J. Biomol. NMR* **11,** 445 (1998).

*30.* P. Andersson, J. Weigelt, and G. Otting, *J. Biomol. NMR* **12,** 435 (1998).

*31.* G. A. Morris and R. Freeman, *J. Am. Chem. Soc.* **101,** 760 (1979).

*32.* A. J. Shaka, J. Keeler, T. Frenkiel, and R. Freeman, *J. Magn. Reson.* **52,** 335 (1983).

*33.* M. McCoy and L. Mueller, *J. Magn. Reson.* **99,** 18 (1992).

*34.* A. Meissner, T. Schulte-Herbrüggen, and O. W. Sørensen, *J. Am. Chem. Soc.* **120,** 7989 (1998).

*35.* M. D. Sørensen, A. Meissner, and O. W. Sørensen, *J. Magn. Reson.* **137,** 237 (1999).

*36.* G. W. Vuister and A. Bax, *J. Magn. Reson.* **98,** 428 (1992).

*37.* D. Yang and L. E. Kay. *J. Am. Chem. Soc.* **121,** 2571 (1999).

*38.* H. Geen and R. Freeman, *J. Magn. Reson.* **93,** 93 (1991).

*39.* L. Emsley and G. Bodenhausen, *Chem. Phys. Lett.* **165,** 469 (1990).

*40.* M. Goldman, *J. Magn. Reson.* **60,** 437 (1984).

*41.* R. Ghose, K. Huang, and J. H. Prestegard, *J. Magn. Reson.* **135,** 487 (1998).

*42.* D. Marion, M. Ikura, R. Tschudin, and A. Bax, *J. Magn. Reson.* **85,** 393 (1989).

*43.* L. E. Kay, G. Y. Xu, T. Yamazaki, *J. Magn. Reson. A* **109,** 129, (1994).

*44.* S. Grzesiek and A. Bax, *J. Am. Chem. Soc.* **115,** 12593, (1993).